Journal of Computer Science

Research Paper

Fine-Tuned and Optimized Transformer-Based Model for EEG Seizure Detection

Puspanjali Mallik[1], Ajit Kumar Nayak[2], Kumar Janardan Patra[3], Rajendra Prasad Panigrahi[4], Getachew Mekuia Habtemaiam[5]

[1]Department of Computer Science and Engineering, Institute of Technical Education and Research, Siksha 'O' Anusandhan (Deemed to be) University, Odisha, India
[2]Department of CS & IT, Institute of Technical Education and Research, Siksha 'O' Anusandhan (Deemed to be) University, Odisha, India
[3]Schools of Computer Sciences, Odisha University of Technology and Research, Odisha, India
[4]Department of computer Science, Institute of Management and Information Technology, BPUT, Odisha, India
[5]Software Engineering Department, Computing College, Debre Berhan University, Ethiopia

Article history
Received: 11 May 2025
Revised: 21 June 2025
Accepted: 8 July 2025

Corresponding Author:
Getachew Mekuia Habtemaiam
Software Engineering Department, Computing College, Debre Berhan University, Ethiopia
Email: getachewmekuria@dbu.edu.et

Abstract: Epilepsy, a widely recognized neurological disorder, results from irregularities in the transmission of electrical impulses among neurons in the brain. Over the last two decades, significant efforts have been made by researchers and clinicians to develop effective methods for its early detection and management. The electroencephalogram (EEG), a non-invasive tool used to monitor brainwave activity, has become a central device in seizure diagnosis. With recent advances, EEG-based analysis is increasingly supported by machine learning and metaheuristic optimization approaches to enhance diagnostic accuracy and efficiency. This research proposes an optimized framework for seizure detection that leverages a Regularized Extreme Learning Adaptive Neuro-Fuzzy Inference System (R-ELANFIS) as the primary classifier. To reduce computational overhead and improve solution accuracy, a hybrid metaheuristic algorithm combining Particle Swarm Optimization (PSO) and Parrot Optimization (PO) is applied to fine-tune the model. The Bonn University EEG dataset, known for its reliable short-term seizure recordings, is used to evaluate system performance. Key classification metrics such as accuracy, sensitivity, and specificity reflect the model's strong predictive capability with accuracy reaching up to 98.3%. The proposed method demonstrates the potential for high-performance EEG-based seizure detection paving the way for future integration with edge computing devices to support remote clinical diagnostics and continuous monitoring in real-world healthcare applications.

Keywords: R- ELANFIS, WPT, Seizure Detection, Sensitivity, Specificity, AUC, 10-fold cross-validation, Transformer, EEGNet.

Introduction

Health issue is an important factor and the complicacies arises related to this needs to face every sort of challenges. In this context, a brain disorder which is otherwise called as epilepsy is a challenging issue and from the past twenty years neurologists and researchers are devising new techniques to detect and predict the presence of disorder signals in brain. Due to this brain disorder, the symptoms observed in outer parts of the body is called as seizure. According to the statistical report of World Health Organization, nearly

50 million of the total population of the world are affected with this disease. This seizure symptoms are of two types: partial or focal seizure and generalized seizure. In case of partial seizure, the disease is observed in a small portion of the brain but in case of generalized seizure, the total brain is affected. Thus, generalized seizure is one type of life-threatening risk-based seizure, happened in form of brain stroke, brain tumour etc. So, the clinical treatment is the only solution to escape from the seizure complexities (Shoka E. et al., 2023). The seizure signals are classified as pre-ictal, ictal and post-ictal. Figure 1 delineates the states of the EEG signal along with the EEG signal representation of CHB-MIT dataset, Bonn University EEG dataset and Kaggle EEG dataset.

Presently, metaheuristic algorithms are emerging as the most powerful and popularly used algorithms which are integrated with machine learning algorithms (Balam V., 2024). There are different types of metaheuristic algorithms such as: nature-inspired, bio-inspired, swarm-inspired and trajectory-based algorithms. In this context, some of the well-known varieties of this kind are: Genetic Algorithms (GA), Particle Swarm Optimization (PSO) Algorithm. Grasshopper Optimization (GO) algorithm, Farmland Fertility (FF) algorithm, Cuckoo Search (CS) Algorithm, Parrot Optimization (PO)Algorithm etc. are devised for reducing complexities in the computational overhead (Ahmad I. et al., 2024).

Although notable progress has been made in seizure detection, several significant limitations remain. Numerous existing techniques involve intricate preprocessing, which hampers their practical use in real-time systems. Some models are tested only on specific datasets, limiting their generalizability across different EEG signals. Others demand high computational power or risk overfitting due to dataset-specific features. Additionally, approaches using complex architectures, like adversarial networks or hybrid methods introduce challenges in tuning and implementation. These issues underline the importance of developing more streamlined, adaptable, and reliable models for effective and wide-ranging seizure detection.

To address the limitations of earlier seizure detection models, we propose an enhanced approach that combines a Transformer-based EEGNet model for feature extraction with the Regularized Extreme Learning Adaptive Neuro-Fuzzy Inference System (R-ELANFIS) classifier for accurate decision-making. To convert EEG signals effectively, we apply the Wavelet Packet Transform (WPT), which captures both time and frequency features. Furthermore, to improve convergence and model precision, we implement a hybrid optimization technique integrating Particle Swarm Optimization (PSO) with the Parrot Optimization (PO) algorithm. This hybrid method fine-tunes the model parameters efficiently reducing training loss and time. Our final results, achieved at 100 epochs, shows an accuracy of 98.3%, sensitivity of 97.8%, specificity of 98.6%, AUC of 0.98, and low loss (0.043) in 24.01 seconds.

The remaining parts of the paper is elaborated in section 2 to section 5. Section 2 includes Literature Review, Section 3 is the core part of the experiment explains about the Methodology used with the sub-sections of 3.1 elaborates flow of work, 3.2 elaborates the features of experimental Bonn EEG dataset, 3.3 states the techniques of EEG data pre-processing, 3.4 states data augmentation, 3.5 states about the proposed Transformer enabled EEG Net model, 3.6 presents the EEG signal to text conversion technique, 3.7 presents the role of RELANFIS in the conversion process, 3.8 presents the feature selection and detection technique and 3.9 presents the fine-tune technique. Section 4 presents experimental results and discussion and section 5 state the conclusion and future scope of the proposed work.

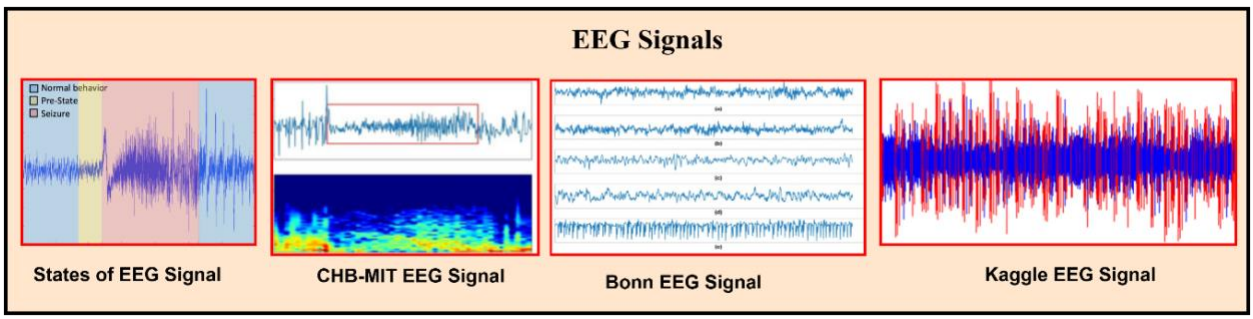

Fig. 1. EEG Signals

Literature Review

Seizure detection represents a challenging research domain that increasingly leverages robust machine learning techniques integrated with metaheuristic optimization approaches. This section reviews relevant prior research that informs the present study.

Signal Processing and Feature Extraction Approaches

Kaushik et al. (2022) proposed a seizure detection technique employing discrete wavelet transform (DWT) sub-bands tested on the Bonn University dataset, utilizing Hjorth parameters to preserve signal efficiency and achieving high classification accuracy. Raghu et al. (2019) implemented DWT followed by Support Vector Machine (SVM) classification for distinguishing seizure signals from normal brain activity, achieving 100% sensitivity on the CHB-MIT dataset and 94.21% accuracy on the Bonn dataset.

Wavelet Packet Transform (WPT), which represents signals in joint time-frequency domains, has been extensively applied to EEG analysis. Xue et al. (2003) and Wu et al. (1996) provided comprehensive explanations of WPT methodology, including detailed decomposition procedures applicable to biomedical signal processing. Andrzejak et al. (2001) established fundamental approaches for representing brain electrical activity patterns to characterize brain states and quantify seizure signal presence.

Deep Learning and Neural Network Approaches

Li et al. (2024) and Liu et al. (2024) developed supervised contrastive learning frameworks for end-to-end seizure detection by optimizing classification boundaries. Their Cos-CNN architecture achieved 75% memory cost reduction through quantization steps and enabled real-time, low-power operation via Field Programmable Gate Array (FPGA) implementation.

Shea et al. (2020) proposed neonatal seizure detection directly from raw multi-channel EEG signals using Convolutional Neural Networks (CNN), compiling a dataset exceeding 834 hours and validating performance against publicly available benchmarks. Recent advances in deep learning for seizure detection have incorporated Long Short-Term Memory (LSTM) networks and attention-based mechanisms (Xu et al., 2024; Ali et al., 2024; Grubov et al., 2024; Yamamoto et al., 2023) to capture temporal dependencies in EEG signals and improve detection accuracy for complex seizure patterns.

Optimization-Based Approaches

Mohapatra et al. (2022) implemented seizure detection using enhanced Atom Search Optimization (ASO) augmented with Lévy flight mechanisms, a stochastic optimization approach for constraint-based problems, achieving superior accuracy, sensitivity, and specificity metrics. The present study builds upon Parrot Optimizer (PO) techniques (Lian et al., 2024) as an enhanced metaheuristic algorithm that improves the velocity and position update mechanisms of traditional Particle Swarm Optimization (PSO) (Gad et al., 2022).

Yang et al. (2021) developed a hybrid PSO-Sparrow Search Algorithm (SSA) approach, demonstrating performance advantages over conventional optimization techniques including Genetic Algorithms (GA), Firefly Algorithm (FFA), and Cuckoo Search. Zhu et al. (2011) devised PSO variants specifically designed for constrained optimization problems, outperforming existing optimization frameworks in benchmark evaluations.

Intelligent Classification Systems

Evolving Local Adaptive Neuro-Fuzzy Inference System (ELANFIS) represents an intelligent fuzzy logic-based classification technique applicable to decision-making and forecasting tasks. Shihabudheen et al. (2017), Tushar et al. (2015), and Yu et al. (2024) implemented Recurrent ELANFIS (R-ELANFIS) integrated with wavelet transform techniques, providing detailed implementation guidelines for intelligent support systems in biomedical applications.

Related Neurological Disorder Detection

Beyond epileptic seizure detection, related neurological disorder identification has received significant attention. Singh et al. (2024) and Divvala et al. (2024) investigated Alzheimer's disease detection methodologies, exploring preventive measures and early symptom identification to facilitate timely intervention. Qiu et al. (2024) emphasized the critical importance of Parkinson's disease detection models, given the life-threatening nature and progressive neurological deterioration associated with this condition. Fıçıcı et al. (2022) specifically addressed temporal lobe epilepsy detection, achieving high accuracy through specialized signal processing approaches.

Table 1 summarizes additional research findings from the reviewed literature (references 28-49), presenting methodological approaches, datasets employed, and performance metrics achieved across various seizure detection studies.

Table 1. Findings from Review Papers

References	Database	Preprocessing Technique	Model	Limitations
(KhalidN.et al., 2024)	UC San Dieg	(PSD)	Gated Recurrent Unit (GRU)	Limited generalizability; tested on a single dataset only
(Islam T., et al., 2023)	TUH EEG corpus database	CWT, Spectrogram, and Wigner-Ville distribution	DenseNet201, DenseNet169,	High computational cost due to multiple complex transforms
(Wang Q, et al., 2023)	Bonn	bandpass filtering and ICA	SVM-KSRC (kernel sparse representation classification)	Kernel methods may not scale well with larger datasets
(Xu Z.et al., 2023)	PhysioNet	Bandpass filtering and ICA	SVM and KNN	Accuracy varies; lacks consistency across datasets
(Khare S. K, et al., 2023)	AZD and NC	(AFAWT)	Adazd-Net	Limited public availability of AZD dataset hinders reproducibility
(Wu T., et al., 2023)	CHB-MIT	Bandpass Filtering Notch Filtering and ICA	Spatial Feature Fused Convolutional Net work (ScNet)	Complex preprocessing may hinder real-time application
(Rukhsar S., et al., 2023)	CHB-MIT	Sequence pooling	Lightweight Convolution Transformer (LCT).	Sequence pooling may lose temporal detail
(Tang S, et al., 2023)	Luoxiong Road Station	Area of Interest (AOI) Analysis and ICA	CNN, LSTM	Specific to activity detection; limited to single scenario
(Jibon F. A, et al., 2023)	CHB-MIT Dataset	Stockwell transform	Linear graph convolutional network (LGCN)	May be overfitted to dataset-specific features
(SiddiqaH. A, et al., 2023)	CHFU, China	Finite Impulse Response	AutoML-based Random Forest estimator	Lower accuracy and may lack robustness
(KatusL.et al., 2023)	West Kiang region of The Gambia	Bandpass filter, ICA	Functional near-infrared spectroscopy (fNIRS)	fNIRS setup not standard in typical EEG studies
(Mane S. A.et al., 2023)	SEED and DEEP	Azimuthal projection	CNN and LSTM	Projection methods may distort spatial features
(Cao J. et al., 2023)	Children's Hospital, Zhejiang University School of Medicine	Z-score normalization	CNN and attenuation mechanism	Over-reliance on normalization techniques
(Cu X. et al., 2023)	Children's Hospital, Zhejiang University	Z-score normalization and Min-Max normalization	CNN	Performance drops on real-world noisy data
(HsiehY. Y. et al., 2022)	CHB-MIT	ICA	Adversarial neural network with Joint-Probability-Discrepancy	Adversarial training adds complexity, needs fine-tuning
(Mallik P. et al., 2024)	CHB-MIT	DWT	LSSVM	Performance drops on real-world noisy data

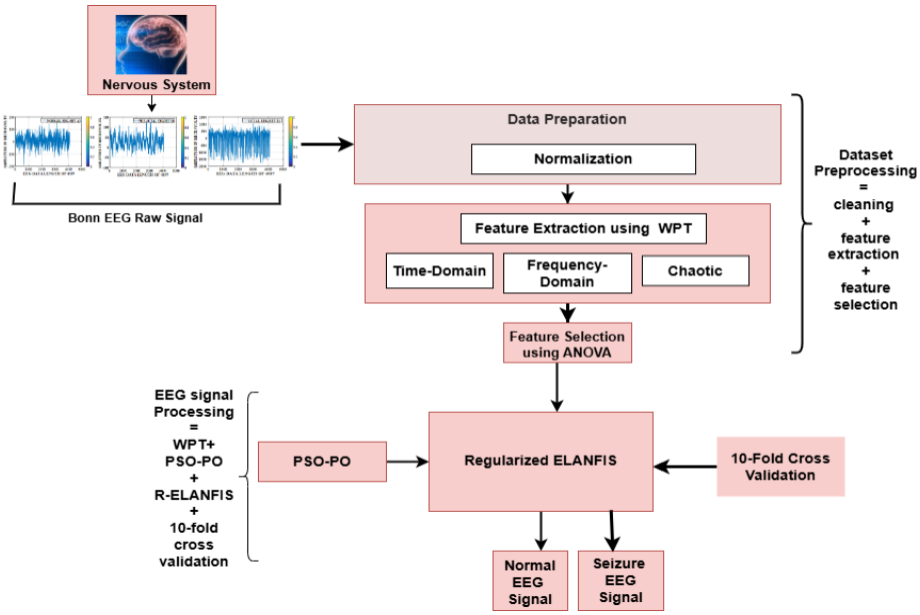

Fig. 2. Steps of the Proposed Model including feature extraction and classification

Methodology

Flow of Work

The process begins with raw EEG signals from the nervous system, followed by normalization and feature extraction using Wavelet Packet Transform (WPT). Features from time, frequency, and chaotic domains are selected via ANOVA. A hybrid model combining PSO-PO and Regularized ELANFIS is applied, and performance is validated through 10-fold cross-validation to classify normal and seizure EEG signals. And the details of the steps are shown in Figure 2.

Clinical Datasets

Bonn university dataset which is collected from Physionet is a publicly available EEG database centre (Andrzejak R. G.et al., 2001). It is a multiclass EEG signal database which is collected from the url: https://www.upf.edu/web/ntsa/downloads/-/asset_publisher/xvT6E4pczrBw/content/2001-indications-of-nonlinear-deterministic-and-finite-dimensional-structures-in-time-series-of-brain-electrical-activity-dependence-on-recording-regi. There arefive classes present in the datasets, class A to class E and each dataset contains 100 txt files with 4096 samples in ASCII format. Class A to class D contain normal signal and class E contains seizure signal. There are 100 channels present with each data set. When the signals are collect5ed from the patient, the electrodes are placed on the surface of the head of the patient positioning inside intracranial regions of the head for the time period of 23.6 seconds. Sample images are shown in Figure 3.

Before preparing the data set for classification, the extracted data samples are then separated into training data and testing data. The time duration for the seizure signal in case of training data is 0.91 hours and testing data is 1.754 hours. We use 51 number of seizure events for training data sample and 86 number of seizure events for testing data sample.

Data Pre-Processing

After successful data collection, the EEG images underwent a structured pre-processing pipeline to improve their quality and consistency. Initially, the images were converted to gray scale, followed by noise reduction using Gaussian and median filtering. Contrast was then enhanced using CLAHE to highlight important features. The images were resized to a standard dimension, and Min-Max normalization was applied to scale pixel values uniformly, ensuring readiness for accurate and efficient analysis. Figure 4 shows the steps of the pre-processed images.

Data Augmentation

To enhance the variability of EEG image samples and improve the model's generalization capability, a comprehensive data augmentation strategy was employed. This process helps mitigate overfitting by introducing diverse visual patterns into the training dataset. The applied transformations included image rotation, horizontal and vertical flipping, resizing, colour jittering, the addition of Gaussian noise, and intensity modifications. These augmentations simulate realistic alterations that could occur in EEG imaging conditions, thereby enabling the model to learn more robust and generalized representations. Examples of these augmented images are illustrated in Figure 5.

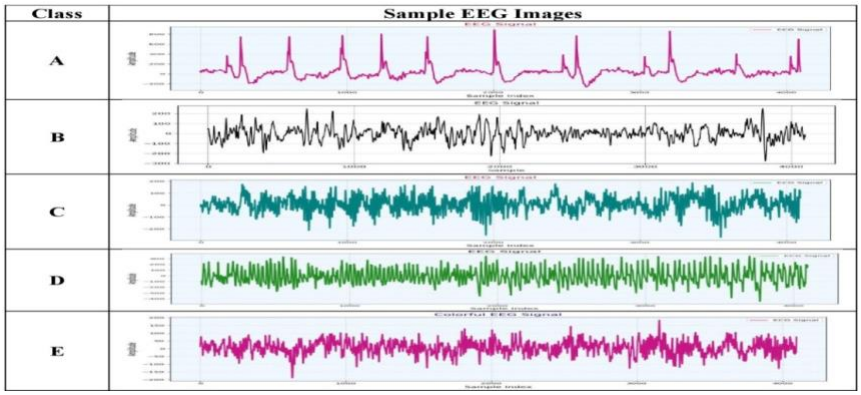

Fig. 3. Bonn dataset EEG signal

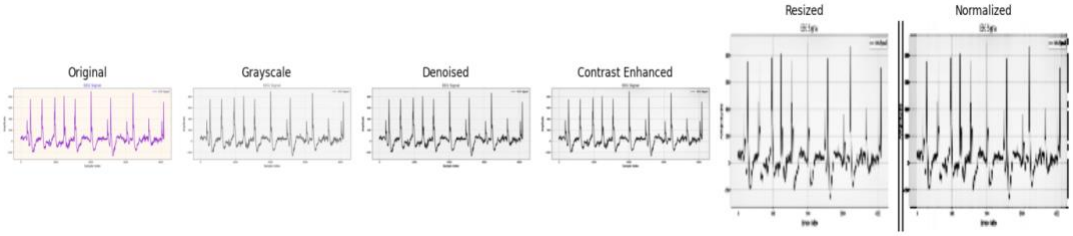

Fig. 4. Pre-processed Images

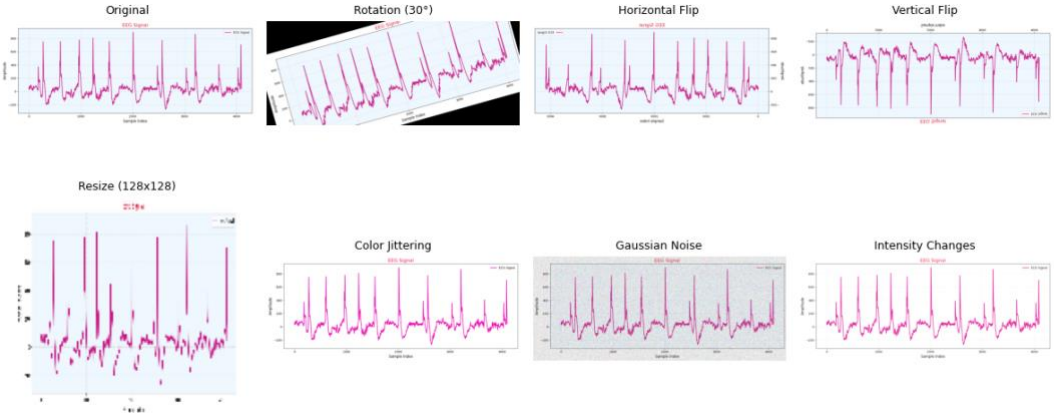

Fig. 5. Sample images of augment data

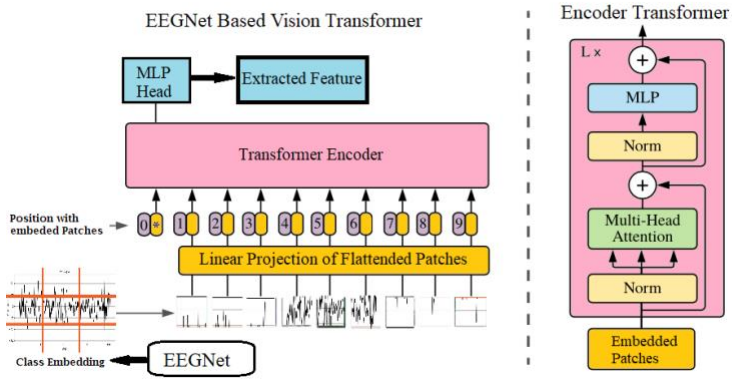

Fig. 6. Transformer based EEGNet architecture

Transformer-Enhanced EEGNet Model

The transformer-enhanced EEGNet model integrates the lightweight design of EEGNet with the attention-based capabilities of transformer architectures. While EEGNet efficiently captures spatial features from multi-channel EEG data through depth wise and separable convolutions, transformers contribute by learning long-term dependencies and global temporal dynamics. This hybrid structure is particularly effective for identifying seizure-related patterns, as it can focus on subtle changes across time and channels. Its ability to model both local and global features makes it a strong choice for accurate and efficient seizure detection using EEG data in real-time applications. Architecture of the model is shown in Figure 6.

Converting EEG Signals to Text Using Key Features

EEG signal data can be converted into a text-based format by extracting and quantifying relevant neurological features. These include variations in amplitude, spike frequency, presence of high-frequency oscillations (HFOs), and signal complexity metrics like entropy or variance. The transformer-EEGNet model first processes EEG input to derive these features. A threshold is applied to isolate significant events, reducing noise and irrelevant fluctuations. The resulting numerical values are then structured as rows in a text file, where each row represents an EEG segment. This output can be directly used for seizure classification or further analysis.

Regularized ELANFIS

To achieve accurate conversion of EEG images into structured text data, a combined framework using Transformer-based EEGNet (TransEEGNet) and the Regularized Extreme Learning Adaptive Neuro-Fuzzy Inference System (Regularized ELANFIS) is proposed. Regularized ELANFIS is an advance version of ANFIS classifier which is an integrated part of the Fuzzy System and machine learning algorithms enriched with language representation and knowledge-based data representation acting as fast as ELM (Shihabudheen et al., 2017). The rules as follows:

$$if\,(x_i\ is\ A_{i1})\ and\ (x_2\ is\ A_{i2}) and\ \cdots\cdots\ and\ (x_n\ is\ A_{in}) \quad (1)$$

$$Rule\ R_1:$$

$$then\ (y_1\ is\ \beta_{i1}), (y_2\ is\ \beta_{i2}), \cdots\cdots\ (y_m\ is\ \beta_{im}) \quad (2)$$

Where $i = 1,2,\cdots L$ (there are L lines used for

$x = [x_1, x_2, \cdots, x_n]^T\ is\ crisp\ input$ and $y = [y_1, y_2 \cdots, y_m]^T$ is crisp output. (3)

$A_{ij}(j = 1,2,\ldots,n)$ are the linguistic variables for the inputs and β_{ik}(k=1,2, …, m) are the crisp variables.

Here the β_{ik} variables can be expressed as

$$\beta_{ik} = \rho_{ik0} + \rho_{ik1}.x_1 + \rho_{ik2}.x_2 + \rho_{iki}.x_n \quad (4)$$

$\rho_{ikl}(l = 0,1,2,\ldots..n)$ are the real valued parameters.

The members grades of the input variables x_j satisfy A_{ij} in the rule I can be expressed as $\mu_{A_{ij}}(x_j)$.

The fuzzy logic expression for the firing string can be represented as

$$w(x) = \mu_{A_{i1}}(x_1) \otimes \mu_{A_i}(x_2) \otimes \ldots \otimes \mu_{A_{in}}(x_n) \quad (5)$$

Here $\otimes$ referes 'and' operator in fuzzy logic.

The normalized firing strength of each rule can be expressed as

$$\overline{w}(x) = \frac{w(x)}{\sum_{i=1}^{L} w_i(x)} \quad (6)$$

'then' part of the expression is linear network having p_{ikl} as its weitht variables. Here the system output is computed as

$$y = \frac{\sum_{i=1}^{L} \beta_i w_i(x)}{\sum_{i=1}^{L} w_i(x)} = \sum_{i=1}^{L} \beta_i\, \overline{w} \quad , \quad ; \quad \beta_i = (\beta_{i1}\,,\ \beta_{i1}\,, \ldots\ \beta_{im}) \quad (7)$$

Figure 7 represents the structure of an ELANFIS classifier

TransEEGNet captures detailed spatial and temporal patterns through its attention-driven architecture, making it effective for detecting seizure-related features. These features are then refined by ELANFIS, which uses fuzzy logic and regularized learning to interpret signal characteristics with greater precision. This integration improves noise resistance, enhances feature clarity, and generates meaningful text-based outputs suitable for clinical evaluation and automated decision support.

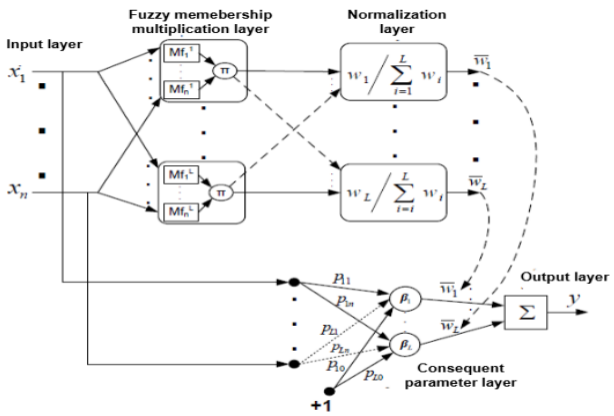

Fig. 7. Structural Representation of ELANFIS

The structural components of ELANFIS have 5 layers, such as input layer, membership function layer, normalization layer, consequent parameter layer and output layer.

Input layer: The nodes present in the input layer are the variables which are connected with the membership function layer

Membership function layer: It is expressed mathematically as

$$g(x_j: a, b, c) = \frac{1}{1+\left|\frac{x_j - c_{ij}}{a_{ij}}\right|^{2b_{ij}}} \quad (8)$$

Where a_{ij}, $2b_{ij}$ and c_{ij} are represented as the premise parameters in fuzzy systems. Here c_{ij} finds the position and a_{ij} and $2b_{ij}$ are used for shape representation. The premise parameters are selected randomly and subsequent parameters ρ_{iki} are learned by least square estimation technique. We trained the model over 100 epochs, observing steady performance improvements and reduced training time per epoch using optimized integration. The training findings of hybrid model values are stored in Table 2 and graphical presentation of training models shown in Figure 8. The findings of the EEG images to text conversion values are stored in Table 3.

Table 2. Training findings of hybrid model

Epoch	Accuracy (AC%)	Sensitivity (SN%)	Specificity (SP%)	AUC	Time Taken (min)
10	96.4	95.8	96.9	0.95	1.5
20	97.1	96.5	97.5	0.96	3.2
40	97.6	97.1	97.9	0.967	6.1
60	97.9	97.4	98.2	0.974	9
80	98.1	97.6	98.4	0.977	11.8
100	98.2	97.7	98.5	0.979	14.5

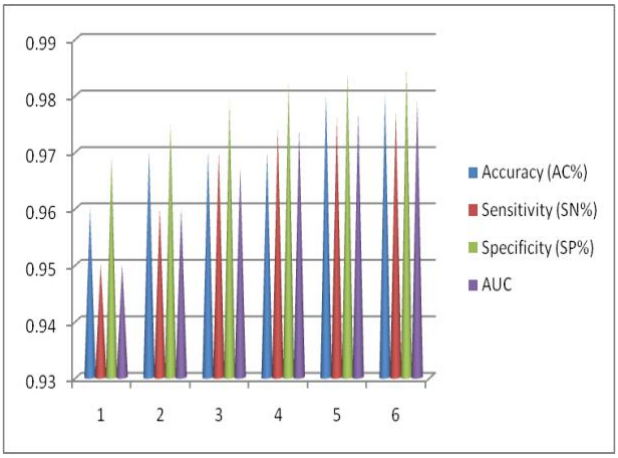

Fig. 8. Graphical presentation of training model

Table 3. EEG Image to Text Conversion Table

Patient_ID	Amplitude Change (μV)	Spike Density (spikes/s)	HFO Rate (Hz)	Entropy	Variance
Threshold	**> 35.0**	**> 2.5**	**> 180.0**	**> 0.75**	**> 1.0**
EEG_001	45.3	3.1	210.5	0.82	1.25
EEG_002	38.7	2.8	185.2	0.76	1.11
EEG_003	51.2	3.6	230.9	0.89	1.39
EEG_004	29.4	1.9	142.7	0.69	0.95
EEG_005	60.8	4.2	256.3	0.94	1.52

Feature Selection and Detection

Wavelet Packet Transform (WPT) is one of the higher forms of Discrete Wavelet Transform (DWT) which consists of Wavelet Packets formed by continuously applying wavelet transforms with the approximation and detail coefficients (Mallik P. et al., 2024). Structurally it is presented as a binary tree representing each node as frequency sub bands. It applies the various decomposition techniques denoising, and signal compression. At first the input signal crossed through wavelet filters. Depending upon the signal strength, specialized nodes are chosen for successive processing and the process repeated. Figure 9 presents the structure of WPT for the discrete sampled signal x.

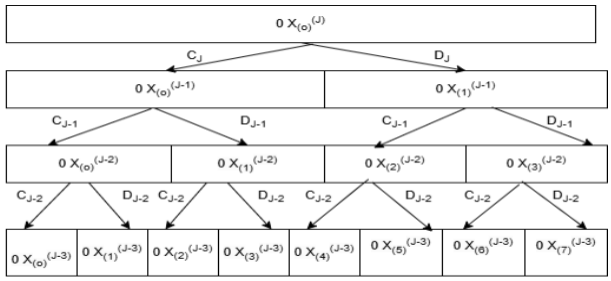

Fig. 9. Structure of a Wavelet Packet Transform Signal

$$x = \left(x_0,\ x_1,,\ldots,x_{2^{j-1}}\ \right)^T = x^{|J|}(0). \quad (9)$$

The $(J-1)^{st}$ level is as per the DWT.

Data crossed through filters.

$${}^0x^{|J-1|}(0) = C_J{}^0x^{|J-1|}(0) = C_J\mathrm{x} \quad (10)$$

$${}^0x^{|J-1|}(0) = D_J{}^0x^{|J|}(0) = C_Jx \quad (11)$$

${}^0x^{|J|}(\tau)$ is used for wavelet packet coefficients at j^{th} level in the τ^{th} band in the decomposition.

The succeeding level of decomposition is

$${}^0x^{|J-2|}(0) = C_{J-1}{}^0x^{|J-1|}(0) \quad (12)$$

$${}^0x^{|J-2|}(1) = D_{J-1}{}^0x^{|J-1|}(0) \quad (13)$$

$$ {}^{0}x^{|J-2|}(2) = C_{J-1}{}^{0}x^{|J-1|}(1) \quad (14) $$

$$ {}^{0}x^{|J-2|}(3) = D_{J-1}{}^{0}x^{|J-1|}(1) \quad (15) $$

The above process repeats until it results one wavelet packet coefficient in each of the bands. With this WPT ensures $2^J - j$ number of bands at each level where $j\epsilon\{J, J-1, \ldots, 0\}$.

Fine-Tune the Model

To enhance the overall efficiency and fine-tune the performance of our proposed model, we integrate a hybrid optimization strategy that combines Particle Swarm Optimization (PSO) with the Parrot Optimizer (PO), referred to as the PSO-PO framework. PSO, inspired by the collective behaviour of social swarms, is widely used due to its simplicity, low computational burden, and effective convergence characteristics. It operates by updating particle positions based on shared information within the swarm, making it suitable for solving a broad range of optimization problems. However, in complex and high-dimensional search spaces, PSO can suffer from premature convergence and get trapped in local optima. To mitigate this limitation, we incorporate the Parrot Optimizer (PO), a relatively novel metaheuristic inspired by the intelligent behavioural patterns of PyrrhuraMolinae parrots. These behaviours, such as foraging for food, maintaining social cohesion, communicating with peers, and reacting to unfamiliar stimuli, are translated into four distinct phases: inspiration, foraging, staying behaviour, and natural response to strangers. By embedding these biologically inspired phases, the PO component strengthens the exploration-exploitation balance of the hybrid model.

The integration of PSO and PO allows the optimization process to maintain diversity in the population, escape local minima, and achieve global convergence more effectively. This hybrid PSO-PO approach significantly reduces training time, enhances parameter tuning accuracy, and improves the model's robustness across varying datasets. Moreover, it contributes to computational efficiency and cost-effectiveness making it well-suited for large-scale biomedical applications where precision and performance are critical. Thus, the PSO-PO optimizer not only fine-tunes the learning process but also adds scalability and reliability to the system's deployment in real-world scenarios.

Mathematical Model of PSO-Parrot Optimization (PO) Algorithm

Population initialization is expressed as

$$ X_i^0 = lb + rand(0,1).(ub - lb) \quad (16) $$

$X_i^0$is the position of ith parrot in initial phase where lb is the lower bound and ub is the upper bound. $rand(0,1)$ is the random number in between 0 and 1.

Foraging Behaviour

It is expressed as

$$ X_i^{t+1} = (X_i^t - X_{best}).Levy(dim) + rand(0,1).\left(1 - \frac{t}{Max_{itr}}\right)^{\frac{2t}{Max_{itr}}}.X_{mean}^t \quad (17) $$

where X_i^t is the current position, X_i^{t+1} is the next position, X_{mean}^t is the average location, and $Levy(D)$ is the Levy distribution.

The average location is expressed as

$$ X_{mean}^t = \frac{1}{N}\sum_{k=1}^{N} X_k^t \quad (18) $$

The Levy distribution is expressed as

$$ \begin{cases} Levy(\text{dism}) = \frac{\mu.\sigma}{|v|^{\frac{1}{\gamma}}} \\ \mu \sim N(0, dim) \\ v \sim N(0, dim) \\ \sigma = \left(\frac{\tau(1+\gamma)\cdot sin\left(\frac{\pi\gamma}{2}\right)}{\tau\left(\frac{1+\gamma}{2}\right)\cdot\gamma\cdot 2^{\frac{1+\gamma}{2}}}\right)^{\gamma+1} \end{cases} \quad (19) $$

Staying Behaviour

It is an immediate change in the looks of the parrot towards the owner's body for a certain amount of time.

$$ X_i^{t+1} = X_i^t + X_{best}.Levy(dim) + rand(0,1) \cdot ones(1.dim) \quad (20) $$

Communicating Behaviour

It is expressed as (21)

$$ X_i^{t+1} = \begin{cases} 0.2 \times rand(0,1) \times \left(1 - \frac{t}{Max_{itr}}\right) \times (X_i^t - X_{mean}^t),\ P \le 0.5 \\ 0.2 \times rand(0,1) \times exp\left(-\frac{t}{rand(0,1)\times Max_{itr}}\right), P > 0.5 \end{cases} $$

Where $0.2 \times rand(0,1) \times \left(1 - \frac{t}{Max_{itr}}\right) \times (X_i^t - X_{mean}^t)$ expresses the technique of an individual to join in the group.

$0.2 \times rand(0,1) \times exp\left(-\frac{t}{rand(0,1)\times Max_{itr}}\right)$ expresses the way of an individual to fly away after communication.

Fear of Stranger's Behaviour

Birds maintain distance when feel someone unfamiliar to keep them safe from unwanted danger.

$$ X_i^{t+1} = X_i^t + rand(0,1) \cdot cos\left(0.5\pi \cdot \frac{t}{\frac{2}{Max_{iter}}}\right) \cdot (X_{best} - X_i^t) - \cos(rand(0,1)\cdot\pi) \cdot \left(\frac{t}{Max_{iter}}\right)^{\frac{2}{t}} \cdot (X_i^t - X_{best}) \quad (22) $$

Algorithm 1: Pseudocode of the PSO-PO Algorithm

Initialize the swarm and parrot parameters
Initialize the position X_{best}
For i=1: Max_{itr}
  For i=1: N
  Find X_{best} of each particle
    $v_i^{t+1} = \omega v_i^t + c_1 r_1 \left(p^t{}_{best_i} - x_i^t\right) + c_2 r_2 (g^t{}_{best} - x_i^t$ // velocity update in PSO
    $x_i^{t+1} = x_i^t + v_i^{t+1}$ // Position update in PSO
    If stopping criteria meets
    X_{best}= Best position
    Else
      k=randi(1,4) // Parrot optimization
      If k==1 // Foragingbehavior

$$X_i^{t+1} = (X_i^t - X_{best}).Levy(dim) + rand(0,1).\left(1 - \frac{t}{Max_{itr}}\right)^{\frac{2t}{Max_{itr}}}.X_{Mean}^t$$

      Else if k==2 // Staying behavior

$$X_i^{t+1} = X_i^t + X_{best}.Levy(dim) + rand(0,1) \times ones(1.dim)$$

      Else if k==3 // Communicating behavior

$$X_i^{t+1} = \begin{cases} 0.2 \times rand(0,1) \times \left(1 - \frac{t}{Max_{itr}}\right) \times (X_i^t - X_{mean}^t), P \le 0.5 \\ 0.2 \times rand(0,1) \times exp\left(-\frac{t}{rand(0,1) \times Max_{itr}}\right), P > 0.5 \end{cases}$$

      Elseif k==4 // The fear of stranger's behavior

$$X_i^{t+1} = X_i^t + rand(0,1) \cdot cos\left(0.5\pi \cdot \frac{t}{Max_{iter}}\right) \cdot (X_{best} - X_i^t) - \cos(rand(0,1) \cdot \pi) \cdot \left(\frac{t}{Max_{iter}}\right)^{\frac{2}{Max_{iter}}} \cdot (X_i^t - X_{best})$$

    end
  end
Return X_{best}

Table 4. Training table for the proposed fine-tuned model

Epoch	Accuracy (AC%)	Sensitivity (SN%)	Specificity (SP%)	AUC	Loss	Time Taken (sec)
10	96.2	95.5	96.7	0.94	0.136	2.9
20	96.9	96.1	97.2	0.955	0.112	8.31
40	97.5	96.8	97.8	0.965	0.089	12.02
60	97.9	97.3	98.2	0.972	0.071	15.99
80	98.1	97.6	98.4	0.976	0.057	19.64
100	98.3	97.8	98.6	0.98	0.043	24.01

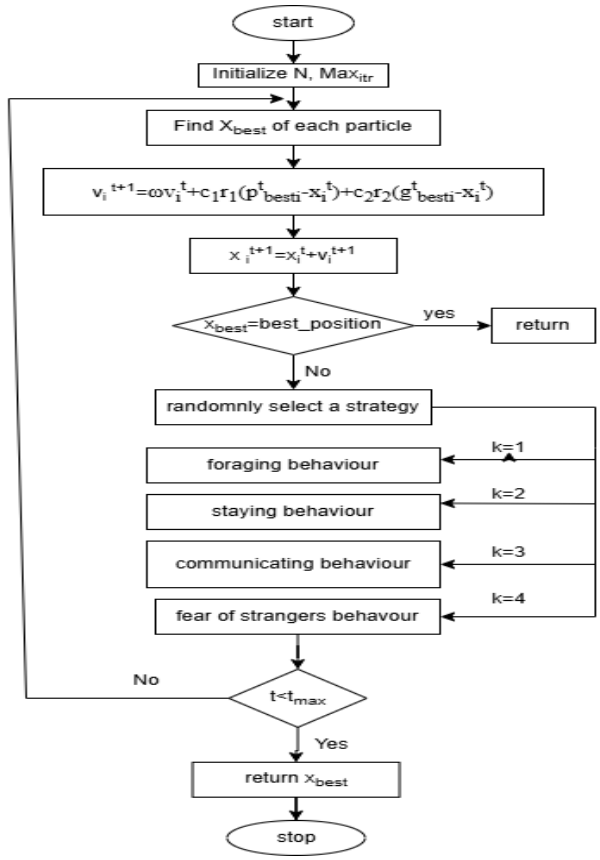

Fig. 10. Flowchart of the Proposed PSO-PO Model

Figure 10 delineates the sequence of steps of the proposed model by means of a flowchart and table 4 stores the values of the training data of the proposed fine-tuned model.

Results and Discussion

The implementation and training of the proposed WPT-PSO-PO-RELANFIS model were carried out on a high-performance computing system to ensure efficient execution and accurate convergence. The system was equipped with an Intel Core i7 11th Generation processor, 32 GB of RAM, and an NVIDIA GeForce RTX 3080 GPU with 10 GB of dedicated memory for accelerated computation. The model was developed using Python 3.9 in a TensorFlow and Keras environment, executed on Ubuntu 20.04 LTS. All experiments were run with CUDA and cuDNN support to leverage GPU-based parallel processing and reduce training time.

To train the proposed model effectively, we initially collected a total of 4,096 EEG images. To enhance the dataset's diversity and improve model generalization, we applied six augmentation techniques, resulting in an expanded dataset of 28,672 images. This enriched dataset was then divided into training, testing, and validation sets using a 70:15:15 ratio. This ensures that the model is trained on a large portion of the data while also being evaluated and validated on separate subsets to prevent overfitting. Table 5 illustrates the dataset distribution across each category.

Table 5. Splitting with ratio

Set	Percentage	Number of Images
Training	70%	20,070
Testing	15%	4,301
Validation	15%	4,301
Total	100%	28,672

The result analysis of this experiment is performed by means of measurement performance parameters expressed as follows.

Suppose $\propto 1, \beta 1, \gamma 1$, and $\delta 1$ are notations for true positive, true negative, false positive and false negative values. Then

$$\text{Accuracy(AC\%)} = \frac{\propto 1+\beta 1}{\alpha 1+\beta 1+\gamma 1+\delta 1} \times 100\% \quad (23)$$

$$\text{Sensitivity(SN\%)} = \frac{\alpha 1}{\alpha 1+\delta 1} \times 100\% \quad (24)$$

$$\text{Specificity(SP\%)} = \frac{\beta 1}{\beta 1+\gamma 1} \times 100\% \quad (25)$$

$$PositivePredictedValue(PPV) = \frac{\alpha 1}{\alpha 1+\gamma 1} \times 100\% \quad (26)$$

$$\text{Matthews Correlation Coefficient (MCC)} = \frac{\alpha 1 \times \beta 1 - \gamma 1.\delta 1}{\sqrt{(\alpha 1+\beta 1) \times (\alpha 1+\delta 1) \times (\beta 1+\gamma 1) \times (\beta 1+\delta 1)}} \times 100\% \quad (27)$$

Table 6 presents the performance parameters of the Bonn EEG dataset using hybridised PSO-PO algorithm with WPT feature extraction method and R-ELANFIS classifier.

Table 6. Measurement performances of different datasets

Performance Computation of different methods of the Bonn University dataset						
Proposed PSO-PO-WPT-RELANFIS Method						
EEG dataset	**AC (%)**	**SN (%)**	**SP (%)**	**PPV (%)**	**MCC (%)**	**AUC (%)**
A-E	98.3	97.8	98.6	92.6	98.5	0.98
C-E	93.8	94.8	92.9	93.6	90.5	0.91
A-D-E	91.3	91.6	84.8	98.4	85.1	0.94
AB-CD-E	84.9	89.90	85.6	97.7	78.6	0.92
ABCD-E	92.0	94.8	90.5	88.6	83.4	0.95

Table 7. 10-fold Validation Over Our Proposed Model To Validate

Fold	Accuracy (AC%)	Sensitivity (SN%)	Specificity (SP%)	AUC	Time Taken (s)
2	97.4	96.9	97.6	0.962	150
3	97.6	97.1	97.8	0.965	180
5	97.9	97.4	98	0.968	210
7	98.1	97.6	98.2	0.973	240
9	98.2	97.7	98.5	0.98	270
10	98.3	97.8	98.6	0.98	300

To evaluate the generalization ability of the WPT-PSO-PO-RELANFIS model, k-fold cross-validation was employed. The dataset was divided into k subsets, and the model was trained k times, each time using a different subset as the validation set. This method helps to ensure robust performance and prevents overfitting. Table7 stores the performance values of the proposed model and Table 8 stores the performance comparison values with existing algorithms.

Table 8. Comparison with existing algorithms

Optimization Algorithms	AC (%)	SN (%)	SP (%)	AUC (%)
GA	87.51	71.5	74.97	0.695
PSO	73.5	74.42	8.240	0.760
BBO	71.3	65	76.47	0.745
FPA	97.23	96.49	98.67	0.972
GWO	95.5	96.3	94.84	0.965
BA	94.33	95.77	91.56	0.943
FA	96.8	93.25	91.12	0.93
CS	94.3	96.44	91.4	0.934
MFO	92.7	94.38	90.88	0.928
Proposed WPT-PSO-PO-RELANFIS	98.3	97.8	98.6	0.98

For ensuring the validation of our proposed work, the measurement performances of our proposed model again compared with the recent research framework and the models added with their findings are stored in Table 9.

Table 9. Performance comparison of the Proposed method with existing methods

Authors	Methods	Dataset	Measurement Parameters		
			AC (%)	SN (%)	SP (%)
(Mathew J. et al., 2023)	Variational Mode Decomposition+root squared zeroth moment	TUH	97.9	97.5	98
		HUP	90.7	90	91.4
(Zhang W. et al., 2023)	Multibit local neighborhood difference pattern +Artificial Rabbits Optimization	Children's Hospital, Zhejiang	97.18	97.03	97.43
(QiuS. et al., 2022)	LSN+1D CNN	CHB-MIT	97.19	96.44	96.2
(Shayeste H. et al., 2022)	Heterogeneous Recurrence Analysis	CHB-MIT	98.5	99.7	99.4
		ABMC	98.5	97.9	98.5
(Zhao W. et al., 2023)	EMA-GHE+RF+SMOTE+FPGA	CHB-MIT	-	95.2	99.3
(Liu S. et al., 2023)	Power spectrum density	CHB-MIT	98.8	-	-
(Yuan, S. et al., 2022)	Adversarial Search + JPDDA	CHZU	98.50	-	-
Proposed Method	**(Best Result Finding) WPT+PSO-PO+R-ELANFIS**	**Bonn**	**98.3**	**97.8**	**98.6**

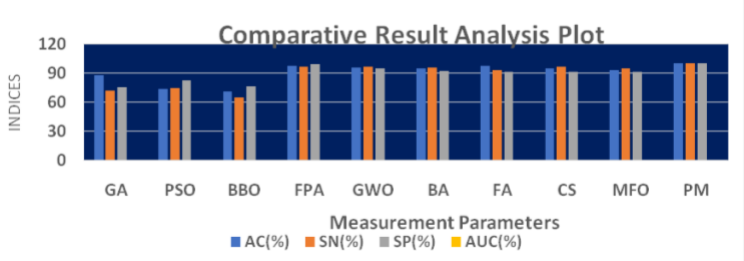

Plot 1. Comparison Result bar chart plot for table 8 values

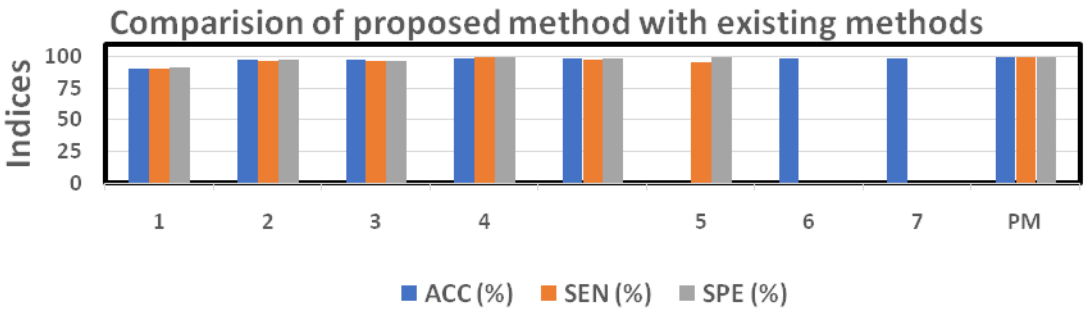

Plot 2. Comparison of Proposed method with existing methods for table 9 values.

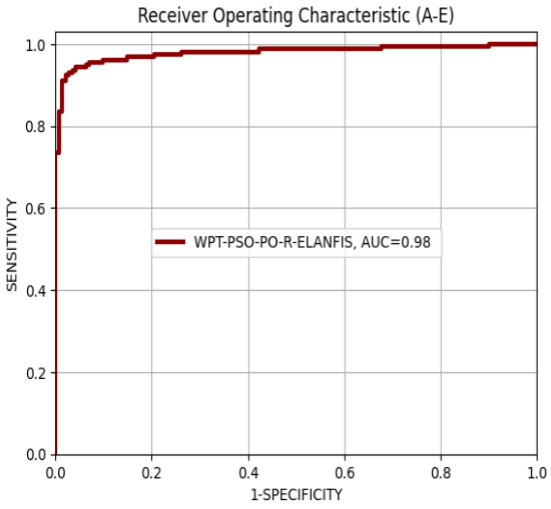

Plot 3. ROC-AUC plot of WPT-PSO-PO-R-ELANFIS for A-E dataset

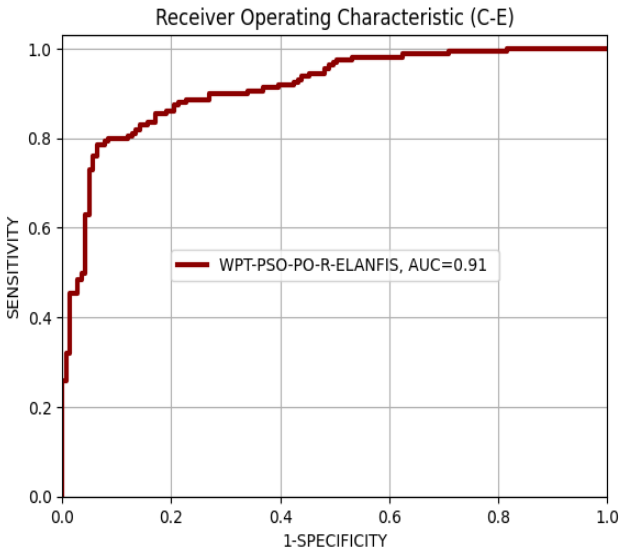

Plot 4. ROC-AUC plot of WPT-PSO-PO-R-ELANFIS for C-E dataset

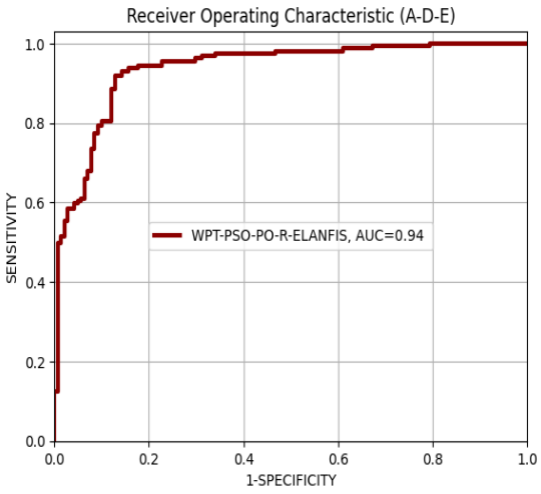

Plot 5. ROC-AUC plot of WPT-PSO-PO-R-ELANFIS for A-D-E dataset

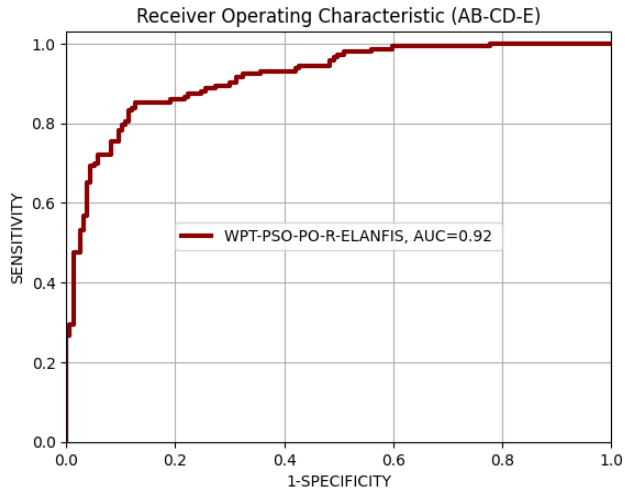

Plot 6. ROC-AUC plot of WPT-PSO-PO-R-ELANFIS for AB-CD-E dataset

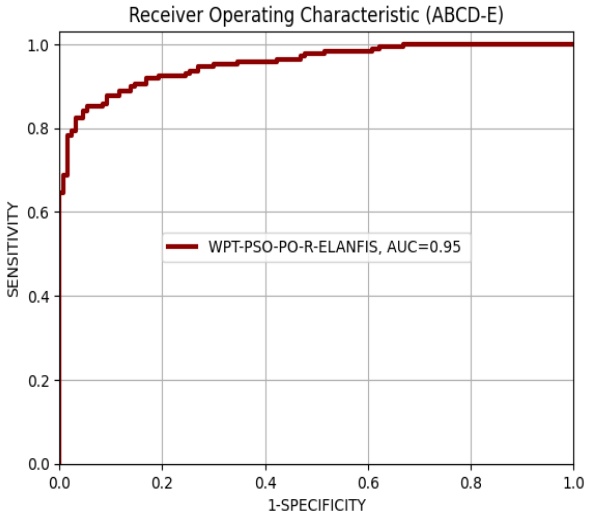

Plot 7. ROC-AUC plot of WPT-PSO-PO-R-ELANFIS for ABCD-E dataset

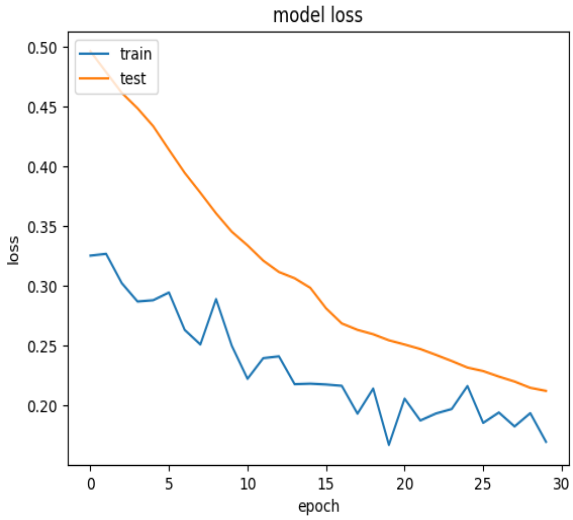

Plot.8 Model loss plot of WPT-PSO-PO-R-ELANFIS for A-E set

The findings of Table 8 values are presented in the form of bar charts in Plot1 and Table 9 values are presented in the form of bar chart in Plot 2.

Plot 3 presents the ROC-AUC curve of A-E dataset, Plot 4 presents the ROC-AUC curve of C-E dataset, Plot 5 presents the ROC-AUC curve of A-D-E dataset and plot 6 presents the ROC-AUC curve of AB-CD-E dataset.

Plots 3 to 8 represent the ROC AUC curve for the mentioned Bonn University EEG dataset according to Table 6.

Model loss curve represents the variation of error and its changes according to the measurement performance of training and testing set outcomes in the course of epochs. The purpose behind this model loss is to analyse the overfitting and underfitting cases. Plot 7 presents the ROC-AUC curve of ABCD-E dataset and the model loss curve of the proposed work for A-E dataset is shown in Plot 8.

Conclusion

Accurate seizure detection is an essential support to the neurologist to aware about the presence of seizure signals in the brain part of the patient. In this case the contribution of the metaheuristic optimization algorithms integrated with the machine learning algorithms plays the lead role to classify the seizure signals. It uses hybridized PSO and parrot optimization algorithm with the measurement outputs of accuracy of 98.3 %, sensitivity of 97.8%, specificity of 98.6 %and ROC-AUC value as 0.98 for the A-E dataset taken from Bonn university EEG dataset. We plan to integrate the edge devices with EEG ecosystem to avail immediate access for our forthcoming experiments.

Data Availability

The dataset used in this study is publicly available from the Bonn University dataset repository. The specific dataset can be accessed at the following link: https://www.upf.edu/web/ntsa/downloads/-/asset_publisher/xvT6E4pczrBw/content/2001-indications-of-nonlinear-deterministic-and-finite-dimensional-structures-in-time-series-of-brain-electrical-activity-dependence-on-recording-regi

Author Contributions

Puspanjali Mallik: Development, implementation, and experimental analysis.
Ajit Kumar Nayak: Supervision, critical insights, and manuscript guidance.
Kumar Janardan Patra: Data preprocessing, model execution, and evaluation.
Rajendra Prasad Panigrahi: Identify research problem, methodology support, and proofreading.
Getachew Mekuria Habtemariam: Collaboration coordination, critical review, and finalization.

References

Ahmad, I., Yao, C., Li, L., Chen, Y., Liu, Z., Ullah, I., & Chen, S. (2024). An efficient feature selection and explainable classification method for EEG-based epileptic seizure detection. *Journal of Information Security and Applications, 80*, 103654. https://doi.org/10.1016/j.jisa.2024.103654

Ali, N. F., Albastaki, N., Belkacem, A. N., Elfadel, I. M., & Atef, M. (2024). A low-complexity combined encoder–LSTM–attention network for EEG-based depression detection. *IEEE Access*.

Andrzejak, R. G., Lehnertz, K., Mormann, F., Rieke, C., David, P., & Elger, C. E. (2001). Indications of nonlinear deterministic and finite-dimensional structures in time series of brain electrical activity: Dependence on recording region and brain state. *Physical Review E, 64*(6), 061907. https://doi.org/10.1103/PhysRevE.64.061907

Balam, V. P. (2024). Systematic review of single-channel EEG-based drowsiness detection methods. *IEEE Transactions on Intelligent Transportation Systems*.

Cao, J., Chen, Y., Zheng, R., Cui, X., Jiang, T., & Gao, F. (2023). DSMN-ESS: Dual-stream multitask network for epilepsy syndrome classification and seizure detection. *IEEE Transactions on Instrumentation and Measurement, 72*, 1–12.

Cui, X., Wang, T., Lai, X., Jiang, T., Gao, F., & Cao, J. (2023). Cross-subject seizure detection by joint-probability-discrepancy-based domain adaptation. *IEEE Transactions on Instrumentation and Measurement, 72*, 1–13.

Divvala, C., & Mishra, M. (2024). Deep learning-based attention mechanism for automatic drowsiness detection using EEG signal. *IEEE Sensors Letters, 8*(3), 1–4.

Ein Shoka, A. A., Dessouky, M. M., El-Sayed, A., & Hemdan, E. E. D. (2023). EEG seizure detection: Concepts, techniques, challenges, and future trends. *Multimedia Tools and Applications, 82*(27), 42021–42051. https://doi.org/10.1007/s11042-023-15244-4

Fıçıcı, C., Telatar, Z., & Eroğul, O. (2022). Automated temporal lobe epilepsy and psychogenic nonepileptic seizure patient discrimination from multichannel EEG recordings using DWT-based analysis. *Biomedical Signal Processing and Control, 77*, 103755. https://doi.org/10.1016/j.bspc.2022.103755

Gad, A. G. (2022). Particle swarm optimization algorithm and its applications: A systematic review. *Archives of Computational Methods in Engineering, 29*(5), 2531–2561.

Grubov, V. V., Nazarikov, S. I., Kurkin, S. A., Utyashev, N. P., Andrikov, D. A., Karpov, O. E., & Hramov, A. E. (2024). Two-stage approach with combination of outlier detection method and deep learning enhances automatic epileptic seizure detection. *IEEE Access*.

Hsieh, Y. Y., Lin, Y. C., & Yang, C. H. (2022). A 96.2-nJ/class neural signal processor with adaptable intelligence for seizure prediction. *IEEE Journal of Solid-State Circuits, 58*(1), 167–176.

Islam, T., Basak, M., Islam, R., & Roy, A. D. (2023). Investigating population-specific epilepsy detection from noisy EEG signals using deep-learning models. *Heliyon, 9*(12), e22533.

Jibon, F. A., Miraz, M. H., Khandaker, M. U., Rashdan, M., Salman, M., Tasbir, A., & Siddiqui, F. H. (2023). Epileptic seizure detection from EEG signals using linear graph convolutional network and DenseNet-based hybrid framework. *Journal of Radiation Research and Applied Sciences, 16*(3), 100607.

Kaushik, G., Gaur, P., Sharma, R. R., & Pachori, R. B. (2022). EEG signal-based seizure detection focused on Hjorth parameters from tunable-Q wavelet sub-bands. *Biomedical Signal Processing and Control, 76*, 103645.

Katus, L., Blasi, A., McCann, S., Mason, L., Mbye, E., Touray, E., & BRIGHT Study Team. (2023). Longitudinal fNIRS and EEG metrics of habituation and novelty detection are correlated in 1–18-month-old infants. *NeuroImage, 274*, 120153.

Khalid, N., & Ehsan, M. S. (2024). Critical analysis of Parkinson's disease detection using EEG sub-bands and gated recurrent unit. *Engineering Science and Technology, an International Journal, 59*, 101855.

Khare, S. K., & Acharya, U. R. (2023). Adazd-Net: Automated adaptive and explainable Alzheimer's disease detection system using EEG signals. *Knowledge-Based Systems, 278*, 110858.

Li, H., Dong, X., Zhong, X., Li, C., Cui, H., & Zhou, W. (2024). End-to-end model for automatic seizure detection using supervised contrastive learning. *Engineering Applications of Artificial Intelligence, 133*, 108665.

Lian, J., Hui, G., Ma, L., Zhu, T., Wu, X., Heidari, A. A., & Chen, H. (2024). Parrot optimizer: Algorithm and applications to medical problems. *Computers in Biology and Medicine, 172*, 108064.

Liu, G., Tian, L., Wen, Y., Yu, W., & Zhou, W. (2024). Cosine convolutional neural network and its application for seizure detection. *Neural Networks, 174*, 106267.

Liu, S., Wang, J., Li, S., & Cai, L. (2023). Epileptic seizure detection and prediction in EEGs using power spectra density parameterization. *IEEE Transactions on Neural Systems and Rehabilitation Engineering, 31*, 3884–3894.

Mallik, P., Nayak, A. K., Mohapatra, S. K., & Swain, K. P. (2024). SH-OSP: A hybrid algorithm using spotted hyena optimizer enabled with optimal stochastic process for epileptic seizure detection. *SN Computer Science, 5*(8), 1168.

Mane, S. A. M., & Shinde, A. (2023). StressNet: Hybrid model of LSTM and CNN for stress detection from EEG signals. *Results in Control and Optimization, 11*, 100231.

Mathew, J., Sivakumaran, N., & Karthick, P. A. (2023). Variational mode decomposition-based moment fusion for the detection of seizure types from scalp EEG measurements. *IEEE Transactions on Instrumentation and Measurement, 72*, 1–12.

Mohapatra, S. K., & Patnaik, S. (2022). ESA-ASO: An enhanced search ability-based atom search optimization algorithm for epileptic seizure detection. *Measurement: Sensors, 24*, 100519.

O'Shea, A., Lightbody, G., Boylan, G., & Temko, A. (2020). Neonatal seizure detection from raw multi-channel EEG using a fully convolutional architecture. *Neural Networks, 123*, 12–25.

Qiu, L., Li, J., Zhong, L., Feng, W., Zhou, C., & Pan, J. (2024). A novel EEG-based Parkinson's disease detection model using multiscale convolutional prototype networks. *IEEE Transactions on Instrumentation and Measurement, 73*, 1–14.

Qiu, S., Wang, W., & Jiao, H. (2022). LightSeizureNet: A lightweight deep learning model for real-time epileptic seizure detection. *IEEE Journal of Biomedical and Health Informatics, 27*(4), 1845–1856.

Raghu, S., Sriraam, N., Temel, Y., Rao, S. V., Hegde, A. S., & Kubben, P. L. (2019). Performance evaluation of DWT-based sigmoid entropy for automated detection of epileptic seizures using SVM classifier. *Computers in Biology and Medicine, 110*, 127–143.

Rukhsar, S., & Tiwari, A. K. (2023). Lightweight convolution transformer for cross-patient seizure detection in multi-channel EEG signals. *Computer Methods and Programs in Biomedicine, 242*, 107856.

Shayeste, H., & Asl, B. M. (2022). Heterogeneous recurrence analysis of imaged-EEG for spatio-temporal epileptic seizure detection. *IEEE Journal of Biomedical and Health Informatics, 27*(1), 351–362.

Shihabudheen, K. V., & Pillai, G. N. (2017). Regularized extreme learning adaptive neuro-fuzzy algorithm for regression and classification. *Knowledge-Based Systems, 127*, 100–113.

Singh, V. K., & Pachori, R. B. (2024). Detection of Alzheimer's disease from EEG signals using improved MCh-EVDHM-based rhythm separation. *IEEE Sensors Letters*.

Tang, S., Xiang, D., Yang, H., Liu, W., He, G., Ma, Z., & Shen, S. (2023). Research on pathfinding cognition in complex underground public space utilizing eye movement and EEG synchronous detection. *Developments in the Built Environment, 16*, 100251.

Tushar, A., & Pillai, G. N. (2015). Extreme learning ANFIS for classification problems. In *2015 1st International Conference on Next Generation Computing Technologies (NGCT)* (pp. 784–787). IEEE.

Wu, T., Fan, Y., Zhong, Y., Cheng, X., Kong, X., & Chen, L. (2023). SCNet: A spatial feature fused convolutional network for multi-channel EEG pathology detection. *Biomedical Signal Processing and Control, 86*, 105059.

Wu, Y., & Du, R. (1996). Feature extraction and assessment using wavelet packets for monitoring of machining processes. *Mechanical Systems and Signal Processing, 10*(1), 29–53.

Xu, J., Yan, K., Deng, Z., Yang, Y., Liu, J. X., Wang, J., & Yuan, S. (2024). EEG-based epileptic seizure detection using deep learning techniques: A survey. *Neurocomputing, 610*, 128644.

Xu, Z., Karwowski, W., Çakıt, E., Reineman-Jones, L., Murata, A., Aljuaid, A., & Hancock, P. (2023). Nonlinear dynamics of EEG responses to unmanned vehicle visual detection with different levels of task difficulty. *Applied Ergonomics, 111*, 104045.

Yamamoto, M. S., Sadatnejad, K., Tanaka, T., Islam, M. R., Dehais, F., Tanaka, Y., & Lotte, F. (2023). Modelling complex EEG data distribution on the Riemannian manifold toward outlier detection and multimodal classification. *IEEE Transactions on Biomedical Engineering, 71*(2), 377–387.

Yang, L., Li, Z., Wang, D., Miao, H., & Wang, Z. (2021). Software defects prediction based on hybrid particle swarm optimization and sparrow search algorithm. *IEEE Access, 9*, 60865–60879.

Yuan, S., Liu, X., Shang, J., Liu, J. X., Wang, J., & Zhou, W. (2022). Automatic seizure detection using logarithmic Euclidean–Gaussian mixture models and improved deep forest learning. *IEEE Journal of Biomedical and Health Informatics, 27*(3), 1386–1396.

Yu, Y., Li, Y., Zhou, Y., Wang, Y., & Wang, J. (2024). A learnable and explainable wavelet neural network for EEG artifacts detection and classification. *IEEE Transactions on Neural Systems and Rehabilitation Engineering*.

Zhang, W., Wu, D., Cao, J., Jiang, L., & Jiang, T. (2023). Multibit local neighborhood difference pattern optimization for seizure detection of West syndrome EEG signals. *IEEE Sensors Journal, 23*(19), 22693–22703.

Zhao, W., Wang, Y., Sun, X., Zhang, S., & Li, X. (2023). IoMT-based seizure detection system leveraging edge machine learning. *IEEE Sensors Journal, 23*(18), 21474–21483.

Zhu, H., Wang, Y., Wang, K., & Chen, Y. (2011). Particle swarm optimization for the constrained portfolio optimization problem. *Expert Systems with Applications, 38*(8), 10161–10169.